Electronic Supplementary Material (ESI) for RSC Advances.

Supporting Information

Sunlight assisted degradation of dye molecules and reduction of toxic Cr(VI) in aqueous medium using magnetically recoverable Fe_3O_4/reduced graphene oxide nanocomposite

Purna K Boruah[a,b], Priyakshree Borthakur[a,b], Gitashree Darabdhara,[a,b], Chaitanya K Kamaja[b,c], Indrapal Karbhal[b,c], Manjusha V. Shelke[b,c], Pallabi Phukan[d], Dulen Saikia[d], Manash R. Das[a,b] *

[a]*Materials Science Division, CSIR-North East Institute of Science and Technology, Jorhat 785006, Assam, India.*

[b]*Academy of Scientific and Innovative Research, CSIR, India*

[c]*Physical and Materials Chemistry Division, CSIR-National Chemical Laboratory, Dr. Homi Bhabha Road, Pune 411008, India*

[d]*Material Science Laboratory, Department of Physics, Sibsagar College, Joysagar 785665, Assam, India*

Preparation of dye and $K_2Cr_2O_7$ solutions

The MG, RhB and MB stock solutions of 10 mM concentration were prepared by dissolving accurately weighted dye molecules in ultrapure water. Similarly, 1 mM stock $K_2Cr_2O_7$ solution was prepared by dissolving accurately weighted solid $K_2Cr_2O_7$ in ultrapure water. From the stock solutions, the required concentrations of the solution were obtained via dilution in accurate proportions.

UV-visible DRS spectra of rGO, Fe_3O_4 and Fe_3O_4/rGO nanocomposite

Important information about the optoelectronic properties of semiconductor is discussed by UV-Visible diffuse reflectance (UV-Vis DRS, PerkinElmer, Lambda 35 UV-Vis Spectrophotometer) spectra of Fe_3O_4/rGO, nanocomposite, Fe_3O_4 nanopowder and rGO sheets are presented in the figure S1. All these nanomaterials display typical absorption peak at UV region of UV-Vis DRS spectra. rGO sheets showed a sharp absorption peak with higher wavelength at UV region in comparison with Fe_3O_4/rGO nanocomposite and Fe_3O_4 nanopowder indicating narrow band gap of rGO sheets. In comparison to the Fe_3O_4 nanopowder, Fe_3O_4/rGO nanocomposite also shows absorption peak at higher wavelength due to the introduction of rGO sheets in nanocomposite, the chemical interaction of the Fe_3O_4 and rGO sheets results in narrowing the band gap of Fe_3O_4.[1]

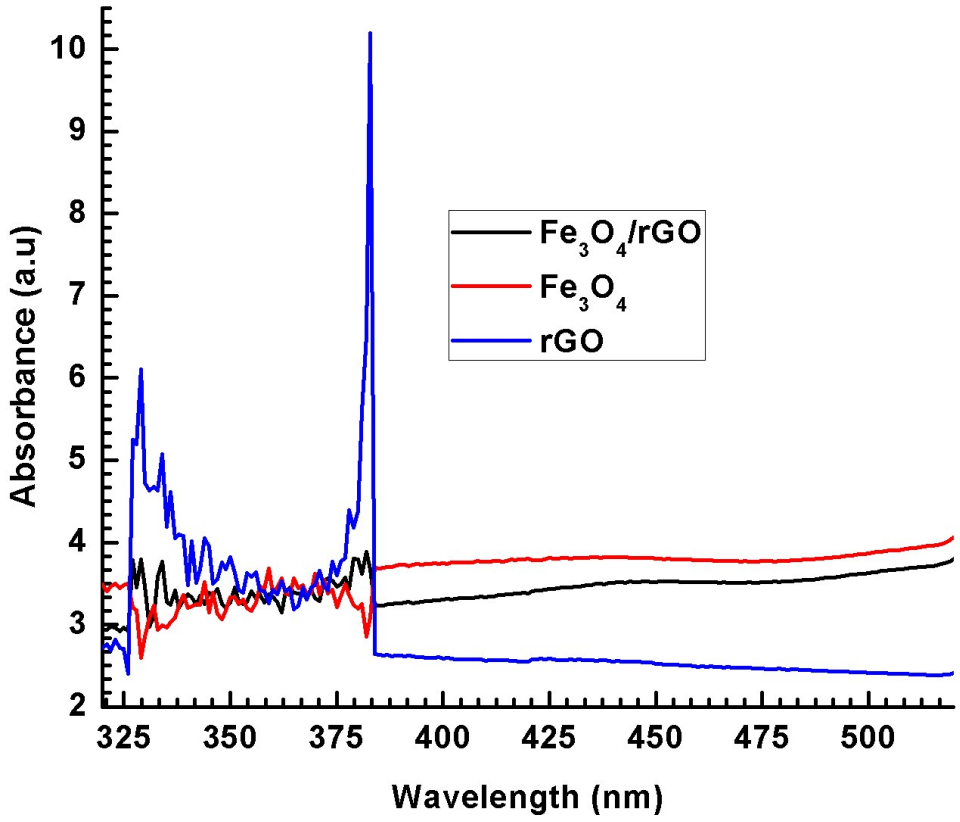

Fig S1. UV-visible DRS spectra of rGO, Fe_3O_4 and Fe_3O_4/rGO

Effect of addition of initial dye concentration on photodegradation

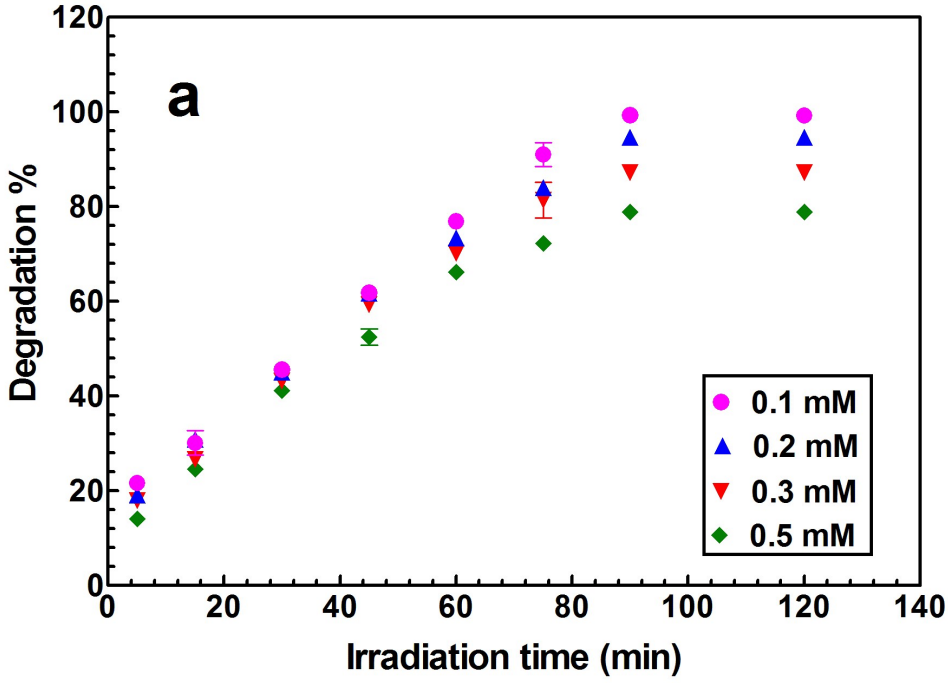

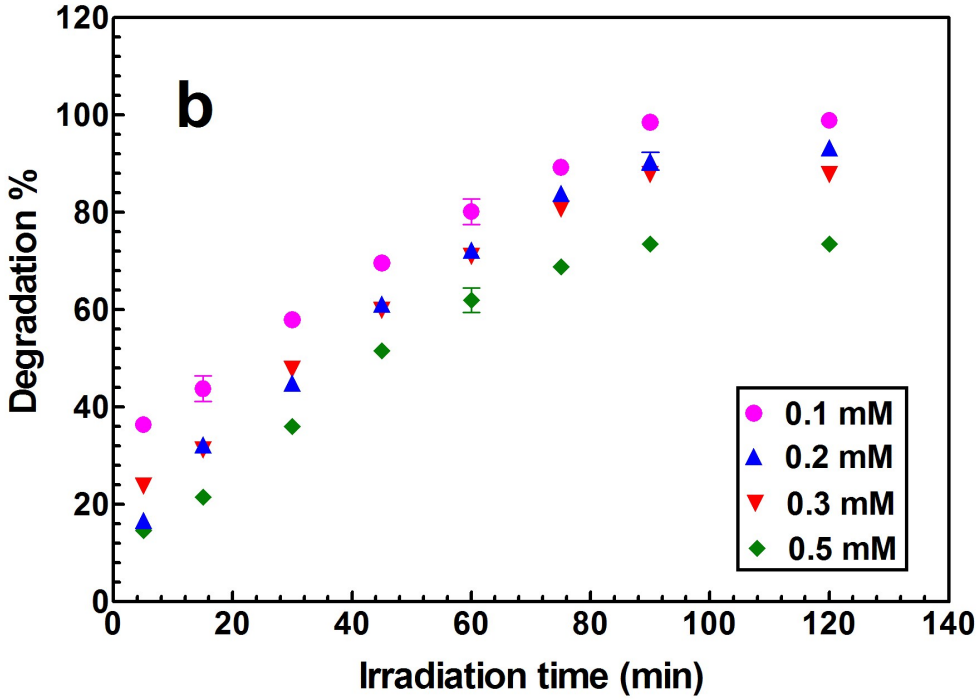

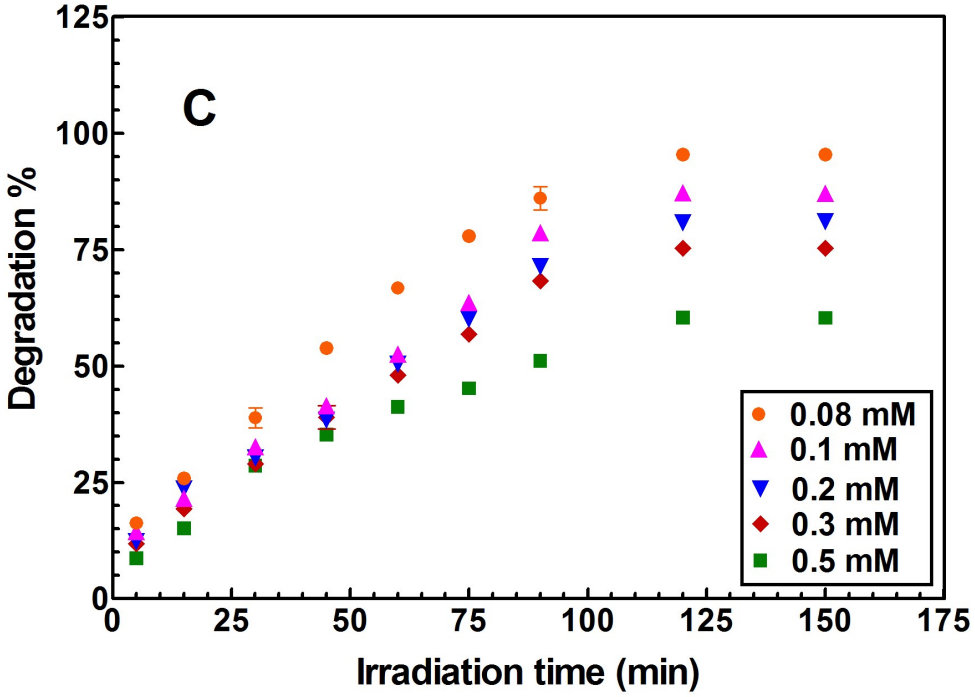

Fig. S2 Photodegradation efficiency of (a) MG, (b) MB and (c) RhB dye molecules at different initial dye concentration (Catalyst loading 0.5 gL^{-1} at pH 5)

Effect of addition of hydrogen peroxide on photodegradation

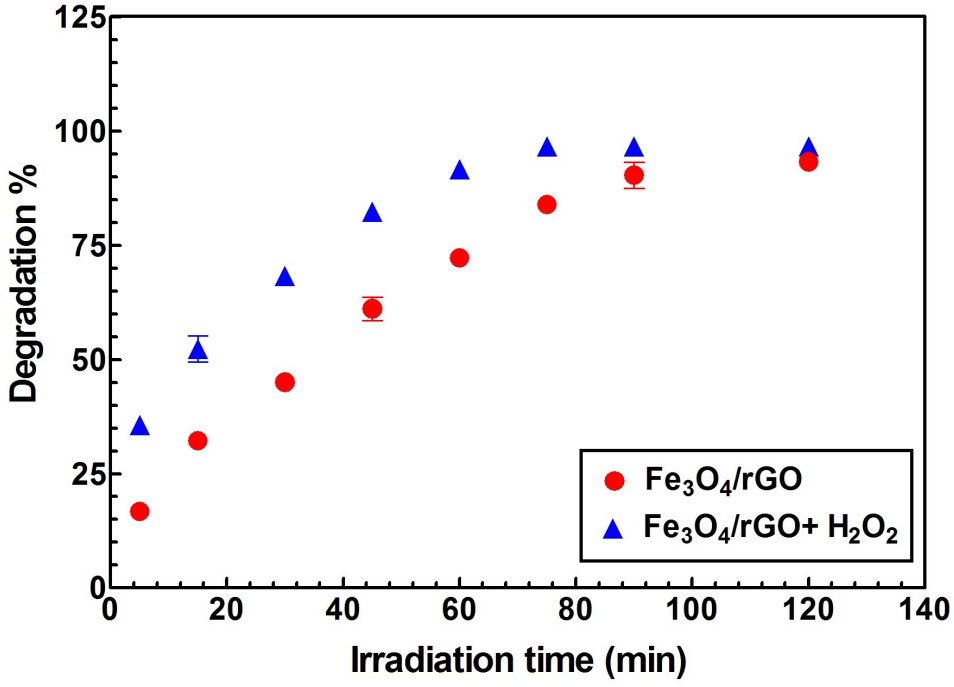

Fig. S3 Effect of addition of H_2O_2 during the photodegradation of MB dye molecule (initial dye concentration 0.2 mM, catalyst loading 0.5gL^{-1}, H_2O_2 concentration 0.02 mM

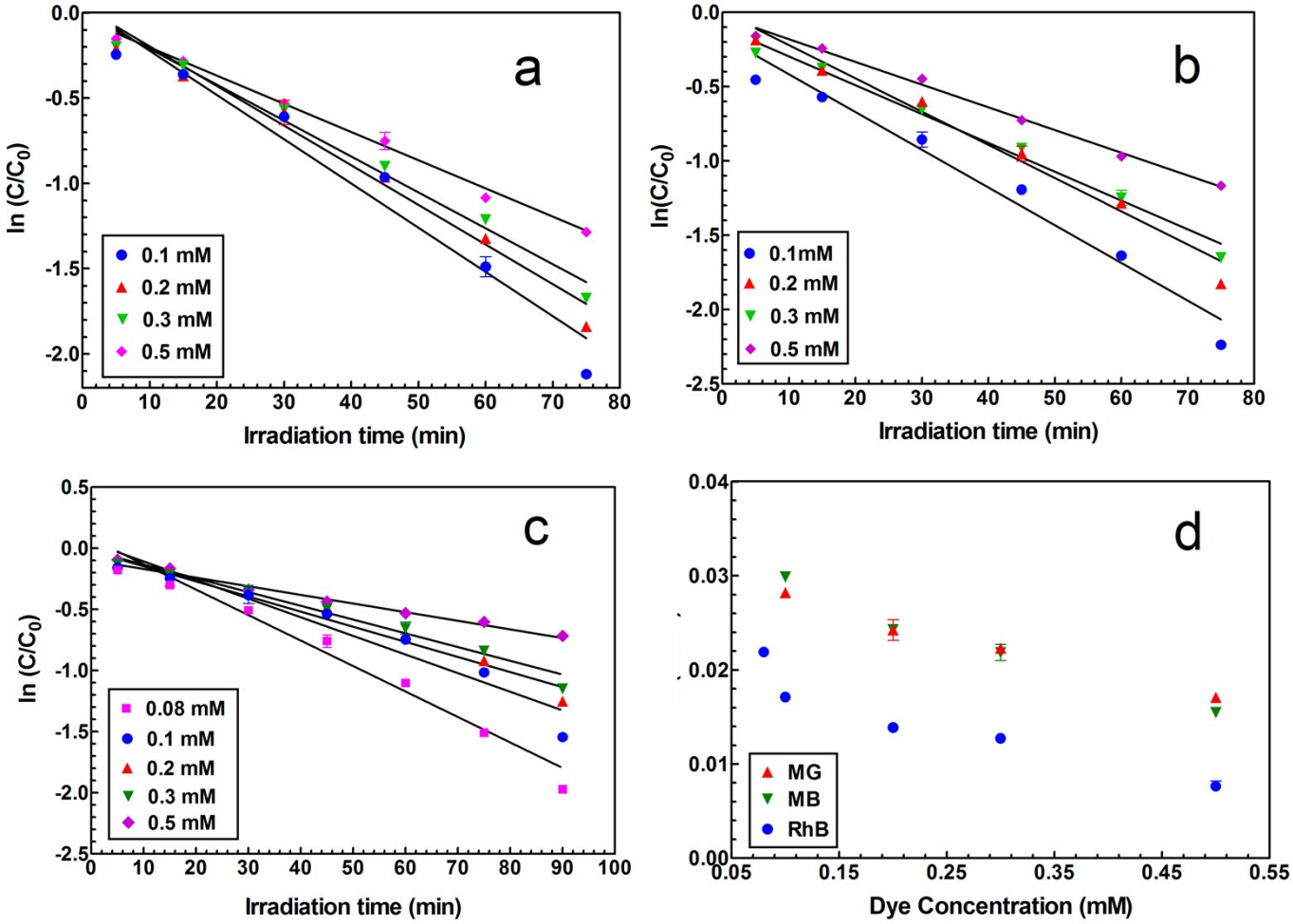

Fig. S4. Langmuir-Hinshelwood pseudo first – order kinetic plots of (a) MG, (b) MB, (C) RhB, and (d) the plots of different initial dye concentration against the pseudo first order rate constant (Catalyst loading 0.5 gL^{-1}, pH5)

Investigation of Intermediate and final products

The initial and the final products in the MG, MB and RhB degradation (dye concentration 0.5 mM, catalyst loading 0.5 gL^{-1}at pH 5) were analyzed using ion chromatography (Metrohm

Compact IC Pro 882, Switzerland). Anion chromatography analysis was carried out for all these dye molecules before and after degradation under sunlight irradiation. It was observed from the Fig. S5 that the peak corresponding to chloride (Cl^-) anion (Cl^- ion existed as a counter ion in aqueous dye solution) appears in the samples that were not subjected to sunlight irradiation. However, the peaks corresponding to the nitrate (NO_3^-) and sulfate (SO_4^{2-}) anions were seen in the degraded samples of the dye molecules. Therefore, it could be inferred that the C–S and C–N bonds in the dye molecules dissociates and sulfur and nitrogen atoms gets oxidized and are directly converted into inorganic harmless NO_3^- and SO_4^{2-} anions and other inorganic molecules like CO_2 and H_2O.

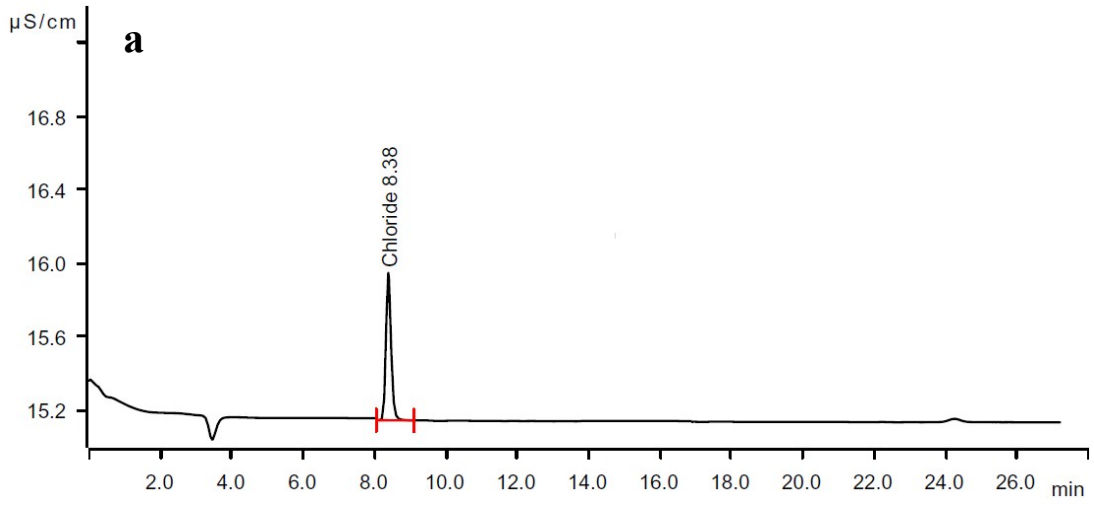

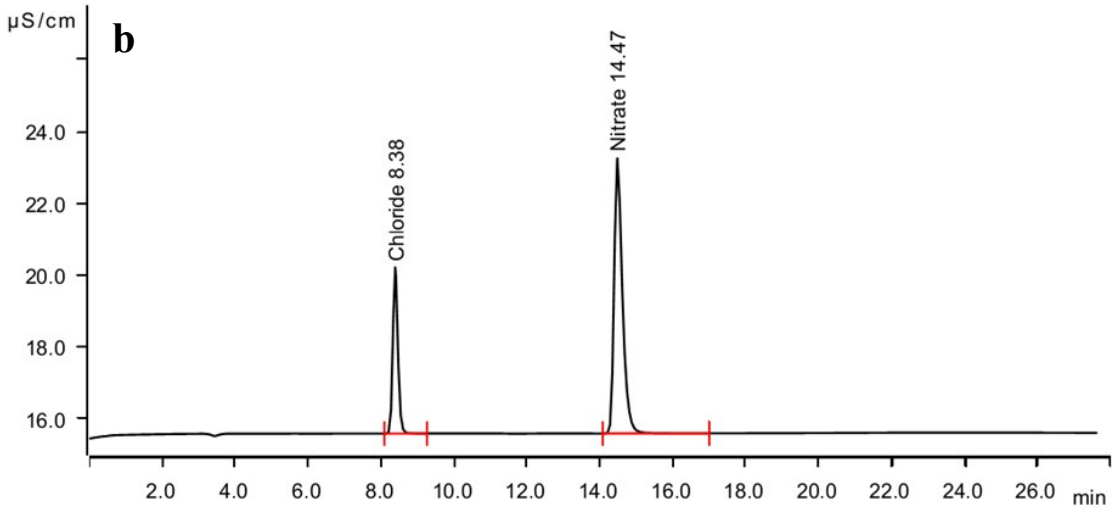
b
µS/cm
24.0
22.0
20.0
18.0
16.0
Chloride 8.38
Nitrate 14.47
2.0
4.0
6.0
8.0
10.0
12.0
14.0
16.0
18.0
20.0
22.0
24.0
26.0
min

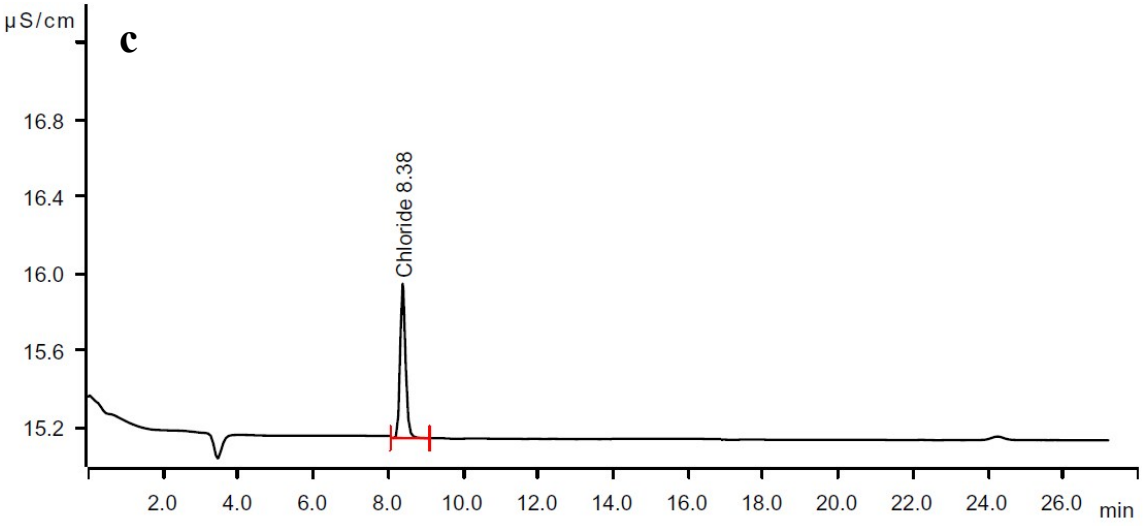
c
µS/cm
16.8
16.4
16.0
15.6
15.2
Chloride 8.38
2.0
4.0
6.0
8.0
10.0
12.0
14.0
16.0
18.0
20.0
22.0
24.0
26.0
min

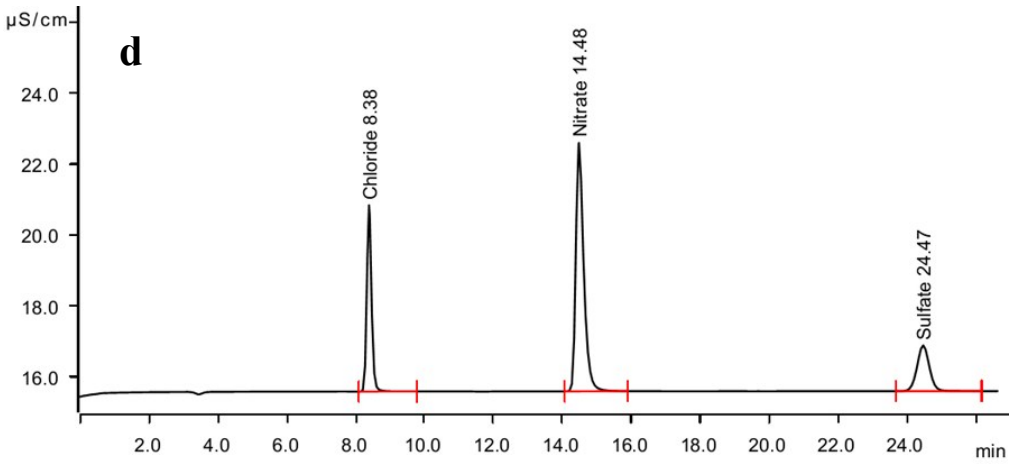
d
µS/cm
24.0
22.0
20.0
18.0
16.0
Chloride 8.38
Nitrate 14.48
Sulfate 24.47
2.0
4.0
6.0
8.0
10.0
12.0
14.0
16.0
18.0
20.0
22.0
24.0
min

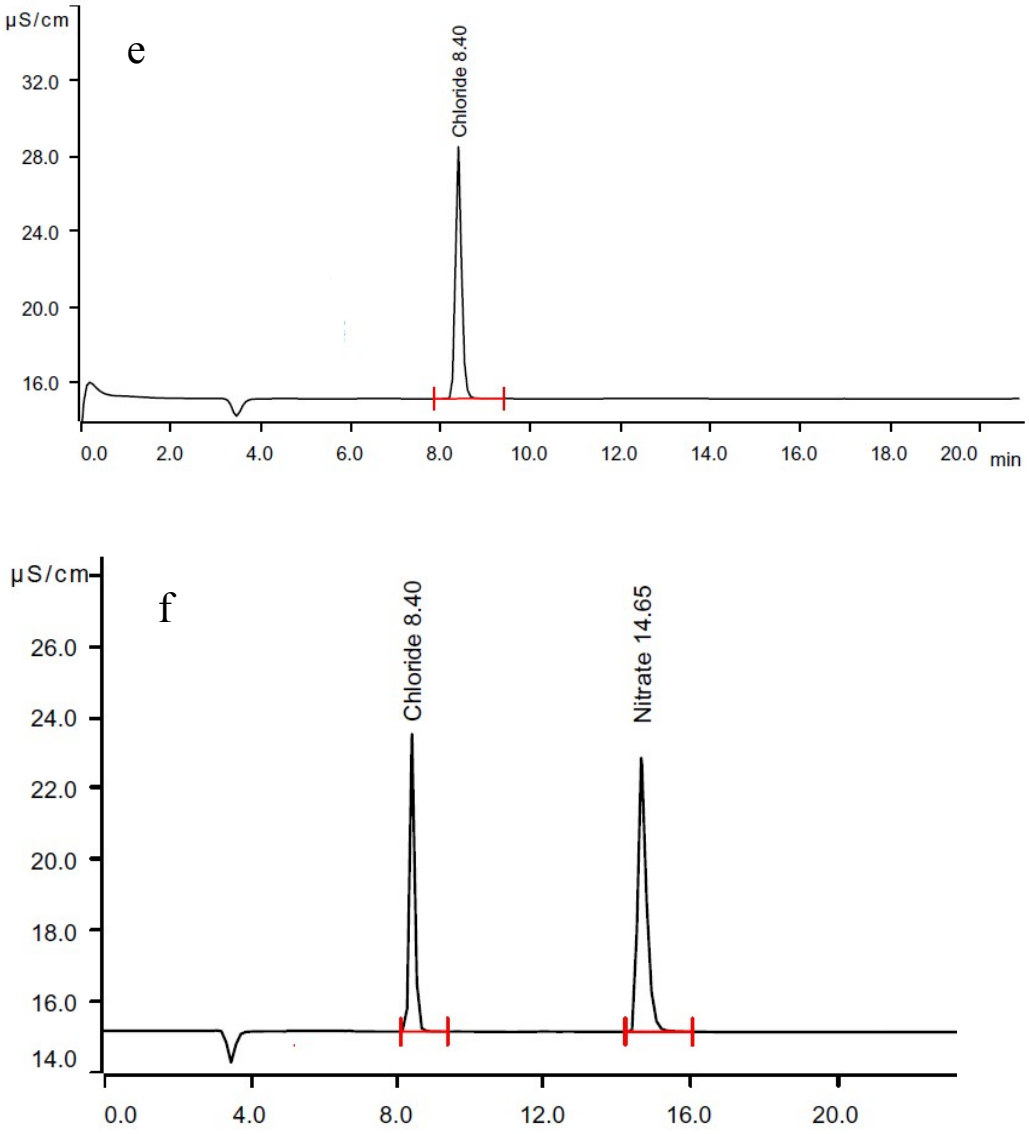

Fig. S5. Ion Chromatogram of MG (a, b), MB (b, c) and RhB (e, f) dye solution before and after photocatalytic treatment.

In order to investigate the intermediate and the final product for the degradation of MG dye molecule, also High Performance Liquid Chromatography (HPLC) analysis was carried out at 626 nm (HPLC, Thermo Scientific 3000, USA). Chromatographic separation was carried out by using C–18 column (250mm × 4.6 mm) at 30 ˚C and mobile phase consisting of 80% acetonitrile and 20% water at a flow rate of 1mL min^{-1}. The matrix peak at 626 nm initially appeared, which decreases along with the irradiation time. The peak corresponding to the 626 nm completely

disappeared after complete degradation of MG dye molecules. Also, no new peaks were identified and thus no byproducts were investigated.

Comparative Cr(VI) reduction

The comparative Cr(VI) photoreduction experiment was performed using 0.08 mM Cr(VI) concentration and catalyst loading 0.5 gL^{-1} at pH 5 under sunlight irradiation during 10 a.m. to 2 p.m. Excellent photoreduction efficiency (96.13%) was achieved for Fe_3O_4/rGO nanocomposite as rGO can act as an electron carrier from the conduction band and hinders electron hole pair recombination in the photoreductionn process (Fig. S6). Therefore, enhanced electron generation was ensured at the conduction band, which is responsible for the Cr(VI) reduction. Due to recombination of photoinduced electron hole pair in the photoreduction process, only 66.12% Cr(VI) reduction efficiency was observed for the Fe_3O_4 nanopowder.[37] However, only 37.31% reduction efficiency was observed for the rGO nanosheets.

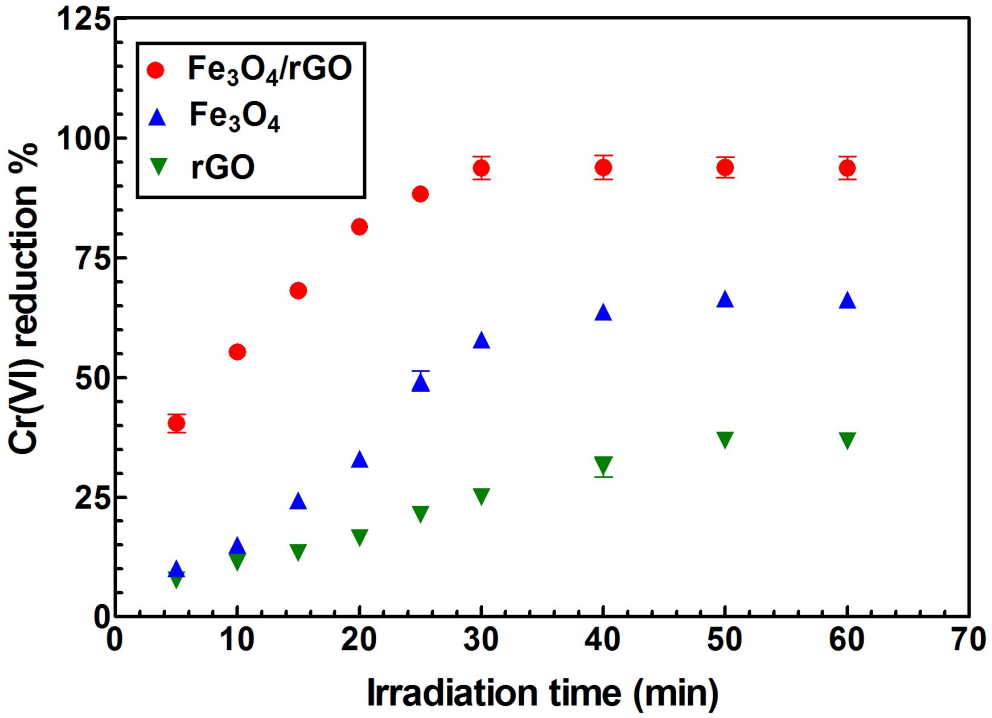

Fig. S6. Comparative photoreduction efficiency of Fe_3O_4/rGO nanocomposite, Fe_3O_4 nanopowder and rGO nanosheets

References:

1. L. Tan, W. Ong, S. Chai and A. R. Mohamed, *Nanoscale Res. Letter* 2013, **8,** 465-474.